Published OnlineFirst February 16, 2017; DOI: 10.1158/0008-5472.CAN-16-2976

Integrated Systems and Technologies

Cancer Research

Lapatinib Resistance in Breast Cancer Cells Is Accompanied by Phosphorylation-Mediated Reprogramming of Glycolysis

Benjamin Ruprecht[1,2], Esther A. Zaal[3], Jana Zecha[1,4,5], Wei Wu[3], Celia R. Berkers[3], Bernhard Kuster[1,2,4,5,6], and Simone Lemeer[1,2,3]

Abstract

HER2/ERBB2–overexpressing breast cancers targeted effectively by the small-molecule kinase inhibitor lapatinib frequently acquire resistance to this drug. In this study, we employed explorative mass spectrometry to profile proteome, kinome, and phosphoproteome changes in an established model of lapatinib resistance to systematically investigate initial inhibitor response and subsequent reprogramming in resistance. The resulting dataset, which collectively contains quantitative data for >7,800 proteins, >300 protein kinases, and >15,000 phosphopeptides, enabled deep insight into signaling recovery and molecular reprogramming upon resistance. Our data-driven approach confirmed previously described mechanisms of resistance (e.g., AXL overexpression and PIK3 reactivation), revealed novel pharmacologically actionable targets, and confirmed the expectation of significant heterogeneity in molecular resistance drivers inducing distinct phenotypic changes. Furthermore, our approach identified an extensive and exclusively phosphorylation-mediated reprogramming of glycolytic activity, supported additionally by widespread changes of corresponding metabolites and an increased sensitivity towards glycolysis inhibition. Collectively, our multi-omic analysis offers deeper perspectives on cancer drug resistance and suggests new biomarkers and treatment options for lapatinib-resistant cancers. *Cancer Res; 77(8); 1842–53. ©2017 AACR.*

Introduction

The receptor tyrosine kinase ERBB2 is overexpressed in 20%–30% of all breast tumors and leads to an increase in the proliferative and invasive potential, which is associated with poor prognosis for patient survival (1). Mechanistically, high levels of ERBB2 cause homodimerization or heterodimerization with other ERBB family members, subsequent autophosphorylation and activation of downstream signaling pathways even in the absence of an activating ligand (2). Pharmacologic efforts directed against ERBB2 activity resulted in the FDA approval of, for example, trastuzumab (3), a mAb that prevents ERBB2 dimerization, and lapatinib (4), a small-molecule EGFR/ERBB2 inhibitor that blocks the kinases' active site. However, despite initially high response rates, breast tumors frequently acquire resistance against targeted therapy. Owing to the early FDA approval of ERBB2-targeted therapies and their clinical prevalence in breast cancer, a wealth of different resistance mechanisms has been described to date.

For example, Liu and colleagues found the overexpression of the receptor tyrosine kinase AXL to be driving lapatinib resistance in the ERBB2-overexpressing breast cancer cell line BT-474 (5). They showed that AXL engaged PIK3, which in turn restored proliferation by recovery of the AKT/MTOR signaling branch. Other examples include signaling switches to other receptor tyrosine kinases [RTKs; EGFR (6), ERBB3 (7), ERBB4 (8), EPHA2 (9), IGF1R (10, 11), MET (12), or MERTK (13), the activation of downstream kinases PRKACA (14), SRC (15–17) or PIK3CA (18) and non-kinase mediated mechanisms (e.g., loss of CDKN1B (19) or increased ESR1 signaling (20)].

Metabolic alterations provide another mechanism by which cancer cells can evade the selective pressure of inhibitor treatment. Overexpression of LDHA (21) as well as increased expression of the glucose deprivation response network (22) are described mechanisms in lapatinib-resistant breast cancer. In addition, two independent studies recently found that small-molecule inhibitor resistance can be mediated by the estrogen-related receptor alpha (ESRRA), which is capable of altering metabolism through transcriptional regulation induced by oncogenic signaling changes (23, 24). Deblois and colleagues showed that MTOR-dependent ESRRA reexpression contributes to lapatinib resistance via increased glutamine metabolism and

[1]Chair of Proteomics and Bioanalytics, Technical University of Munich, Freising, Germany. [2]Center for Integrated Protein Science Munich (CIPSM), Freising, Germany. [3]Biomolecular Mass Spectrometry and Proteomics, Bijvoet Center for Biomolecular Research and Utrecht Institute of Pharmaceutical Sciences, Utrecht University, Utrecht, the Netherlands. [4]German Cancer Consortium (DKTK), Heidelberg, Germany. [5]German Cancer Research Center (DKFZ), Heidelberg, Germany. [6]Bavarian Biomolecular Mass Spectrometry Center, Technical University of Munich, Freising, Germany.

Note: Supplementary data for this article are available at Cancer Research Online (http://cancerres.aacrjournals.org/).

Current address for S. Lemeer: Biomolecular Mass Spectrometry and Proteomics, Bijvoet Center for Biomolecular Research and Utrecht Institute of Pharmaceutical Sciences, Utrecht University, Utrecht, the Netherlands.

Corresponding Authors: Simone Lemeer, Biomolecular Mass Spectrometry and Proteomics, Bijvoet Center for Biomolecular Research, Utrecht University, Padualaan 8, Utrecht 3584 CH, the Netherlands. Fax: 4981-6171-5931; E-mail: S.M.Lemeer@uu.nl; and Bernhard Kuster, kuster@tum.de

doi: 10.1158/0008-5472.CAN-16-2976

Published OnlineFirst February 16, 2017; DOI: 10.1158/0008-5472.CAN-16-2976

Park and colleagues provided evidence for intrinsic resistance of breast cancer cells to PIK3/MTOR inhibition, which is caused by alteration of mitochondrial function and lactate metabolism. Both studies reveal a tight orchestration of kinase signaling, protein expression changes, and metabolic adaption, which clearly highlights the importance of a systems-level understanding of resistance and furthermore suggests the existence of several parallel and targetable alterations, which are codependent.

Mass spectrometry–based technologies nowadays allow for the explorative and large-scale assessment of (phospho)proteins and metabolites, thus rendering the study of such complex associations feasible. Here, we used an established, lapatinib-resistant BT-474 cell line model (5) and applied a combination of proteomics, chemoproteomics, phosphoproteomics, and metabolomics in an effort to globally assess the molecular consequences of lapatinib treatment and resistance. Collectively, our analysis offers a systems-wide view on the molecular mechanisms of resistance and shows that the acquisition is accompanied by many pharmacologically exploitable alterations. Specifically, the data suggest that posttranslational regulation of glycolysis leads to increased metabolic dependence on glucose consumption (glycolytic addiction) in lapatinib resistance. In combination with results from other studies, this observation implies that increased glucose addiction in resistance can occur via multiple different routes. Hence, this phenotype might represent a common and targetable convergence point and, as such, a universal "Achilles' heel" of resistance to ERBB2-targeted therapies in breast cancer.

Materials and Methods

Cell culture and reagents

Parental BT-474 cells and its lapatinib resistant clone BT-474-J4 were received from the Department of Translational Research, GlaxoSmithKline and were grown in DMEM/Ham F-12 medium (Biochrom) supplemented with 15% (v/v) FBS (Biochrom) and 1% (v/v) antibiotic/antimycotic solution (Sigma). The cell line identity of BT-474 cells was confirmed to be 100% by SNP profiling and comparison with a reference database. Resistant BT-474-J4 cells were cultured in the continuous presence of 1 μmol/L lapatinib. Both cell lines were regularly tested for *Mycoplasma* infection. Biological replicates were prepared at different days using a different cell line passage. Lapatinib, dasatinib, and bosutinib were purchased from LC Laboratories, 2-deoxy-D-glucose was purchased from Sigma Aldrich and saracatinib, selumetinib, linsitinib, BMS-387032, SCH-727965, and MK-2206 were purchased from Selleckchem.

Viability and invasion assay

For viability/drug treatment assays, cells were seeded in 96-well plates at a concentration of 4×10^4 cells/well with complete culture medium. Cell viability was measured using the AlamarBlue Cell Viability Assay (ThermoFisher Scientific) according to manufacturer's instructions. For EC_{50} calculations, sigmoidal dose–response curves were fitted using a variable four-parameter nonlinear regression model in GraphPad Prism v.5.01. The invasive potential of parental and resistant BT-474 cell lines was assessed in a transwell assay using BD Matrigel (VWR).

Cell lysis

Prior to harvest, cells were washed two times with PBS. For (phospho)proteome preparation, cells were lysed in 8 mol/L urea, 40 mmol/L Tris/HCl (pH 7.6), 1 × EDTA-free protease inhibitor mixture (complete mini, Roche), and 1 × phosphatase inhibitor cocktail 1, 2, and 3 (Sigma). The lysate was centrifuged at 20,000 × *g* for 45 minutes at 4°C. For kinobead experiments, cells were lysed in 1× CP buffer (50 mmol/L Tris-HCl, pH 7.5, 5% glycerol, 1.5 mmol/L $MgCl_2$, 150 mmol/L NaCl) supplemented with 0.8% NP-40, 1 mmol/L DTT, 25 mmol/L NaF, and freshly added protease and phosphatase inhibitors (5 × phosphatase inhibitor cocktail 1 and 2, Sigma-Aldrich; 1 × phosphatase inhibitor cocktail 3, Sigma-Aldrich; 1 mmol/L Na_3VO_4). CP buffer protein extracts were clarified by ultracentrifugation at 150,000 × *g* for 1 hour at 4°C. Protein concentration for phosphoproteome and kinome samples was determined by the Bradford method [Coomassie (Bradford) Protein Assay Kit, Thermo Scientific) and the cleared lysates were stored at −80°C until further use.

Digestion and dimethyl labeling for phospho- and full proteome preparation

The urea-containing lysate was reduced with 10 mmol/L DTT at 56°C for 30 minutes and alkylated with 55 mmol/L CAA for 30 minutes at room temperature in the dark. The protein mixture was diluted with 40 mmol/L Tris/HCl to a final urea concentration of 1.6 mol/L. Digestion was performed by adding sequencing grade trypsin (Promega) in an enzyme-to-substrate ratio of 1: 100 and incubation for 4 hours at 37°C. Subsequently, another 1: 100 trypsin was added for overnight digestion at 37°C. The next day, samples were acidified with TFA to a pH of 2 and desalted using SepPak columns [C18 cartridges Sep-Pak Vac 1 cc (50 mg), Waters Corp., solvent A: 0.07% TFA, solvent B: 0.07% TFA, 50% ACN]. Dimethyl labeling was performed on column as described previously (25).

Fe-IMAC column enrichment and (phospho)peptide fractionation

Phosphopeptide enrichment was essentially performed as described previously (26). Detailed description of high pH reversed-phase micro-column fractionation can be found in the Supplementary Materials and Methods section. Hydrophilic strong anion exchange fractionation of 300 μg Fe-IMAC column flow through into 24 fractions was performed as described previously (26).

Sample preparation for metabolomics experiments

BT-474 and BT-474-J4 cells were seeded in triplicates on 6-well plates at a density of 4×10^5 cells per well. Extra wells were seeded for cell counting. After 24 hours, media were replaced and after 2, 8, and 24 hours, cells were washed with ice-cold PBS, and metabolites were extracted in 0.25-mL lysis buffer containing MeOH/ACN/ddH_2O (2:2:1). Samples were centrifuged at 16,000 × *g* for 15 minutes at 4°C and supernatants were collected for LC/MS analysis. In addition, the media were sampled 8 and 24 hours after exchange. For this, 10 μL of medium was added to 1 mL of lysis buffer containing MeOH/ACN/ddH_2O (2:2:1) and prepared as described above.

Kinase affinity pull downs

Kinobead pull downs were conducted in a 96-well plate format as described previously (27, 28).

Published OnlineFirst February 16, 2017; DOI: 10.1158/0008-5472.CAN-16-2976

LC/MS-MS measurements

For full- and phosphoproteome fractions, nanoflow LC/MS-MS was performed by coupling an Agilent 1290 (Agilent Technologies) to an Orbitrap Q Exactive Plus mass spectrometer (Thermo Scientific). For kinobead eluates, nanoflow LC/MS-MS was performed by coupling an UltiMate 3000 nano LC system (Thermo Scientific) to a Q Exactive HF mass spectrometer (Thermo Scientific). For metabolomics experiments, LC/MS analysis was performed on a Q Exactive mass spectrometer (Thermo Scientific) coupled to a Dionex Ultimate 3000 autosampler and pump (Thermo, Scientific). Detailed LC and MS parameters can be found in the Supplementary Materials and Methods section.

Statistical analysis

Processing of raw mass spectrometric data was performed using MaxQuant v1.4.0.5 (29). To facilitate further data analysis, the results were either imported into the MaxQuant associated software suite Perseus (v.1.5.0.15; ref. 30) or into Microsoft Excel (Microsoft). Data normalization was performed according to a procedure that will be published elsewhere. A two-sided Student *t* test was used to assess statistical significance. Phosphopeptide and protein *P* values were corrected for multiple testing using a permutation-based 1% FDR cutoff (250 randomizations; S0 of 0.5). Metabolites were quantified using LCQUAN software (Thermo Scientific).

ProteomeXchange accession

The mass spectrometry proteomics data have been deposited to the ProteomeXchange Consortium via the PRIDE partner repository with the dataset identifier PXD004981.

Additional information

Additional information on materials and methods used in this study is provided in the Supplementary Information section.

Results

Mass spectrometry–based multiproteomic profiling of lapatinib action and resistance

With the aim to globally study lapatinib action and lapatinib resistance, we performed a mass spectrometry–based (phospho)proteomic analysis on a previously established cell line model system, consisting of both a lapatinib-sensitive and a lapatinib-resistant cell line (5). Triple dimethyl-labeling of proteome digests in combination with Fe-IMAC column-based phosphopeptide enrichment allowed us to compare the (phospho)proteome of parental cells to cells exposed to 1 μmol/L lapatinib and to lapatinib-resistant cells (Fig. 1A; four independent biological replicates). To gain further insight into protein kinase expression changes, we additionally performed kinase affinity enrichment using kinobeads γ (KBγ) in triplicate (Fig. 1A; ref. 27). The collective dataset (Supplementary Tables S1–S5) comprised quantitative information for >7,800 proteins (Supplementary Fig. S1A and S1B), >300 protein kinases, and >15,000 unique phosphopeptides (>9,800 unique phosphorylation sites; Supplementary Fig. S1C–S1E). The correlation between biological replicates was excellent (average Pearson *R* of >0.98 for phosphopeptides and >0.99 for proteins from replicates of the same condition; Supplementary Fig. S1F and S1G) and principal component analysis (PCA) of the twelve experimental states (three dimethyl channels in four replicates) revealed that the proteome and phosphoproteome samples cluster according to biology rather than batch (Fig. 1B).

Phosphoproteomic analysis of lapatinib mode of action in parental cells

We first analyzed the phosphorylation changes induced by treatment of the parental cell line with 1 μmol/L lapatinib for 30 minutes. To assess statistical significance, a FDR-controlled *t* test (FDR < 0.01, S0 of 0.5) was performed on localized sites (localization probability >0.75) that were observed in a minimum of three biological replicates. Despite the inhibitor's exquisite selectivity, a total of 332 sites (5% of the 6421 sites) changed significantly upon short-term lapatinib treatment (178 sites down and 154 sites up; Fig. 2A). As expected, less than one percent of the measured proteins changed significantly within the same period of time (Supplementary Fig. S2A). Figure 2B shows that the 178 downregulated sites contain several known ERBB2 pathway and protein activity–regulating kinase phosphorylation sites such as ERBB2 pY-1233 ($\log_2$ FC of -1.3; P = of 3.6E−4) or MAPK3 pY-204 ($\log_2$ FC -3.2; P = of 1.2E−08). Enrichment analysis of combined kinase substrates and linear motifs among regulated sites (30) showed strong inhibition of AKT-MTOR-RPS6KB1 and EGFR-MAPK1/3-RPS6KA3 signaling upon lapatinib treatment (Fisher exact test, FDR < 0.01; Supplementary Fig. S2B). The analysis additionally uncovered regulation of receptor tyrosine kinase adaptor proteins such as IRS1/2, SHC1, or GAB2 and the inactivation of central transcription factors such as *JUN* and MYC (Fig. 2C). Global protein interaction analysis of changing phosphoproteins using the STRING database in combination with KEGG annotation of the extracted network confirmed the perturbation of MTOR signaling (FDR = 7.5E−07), ERBB signaling (FDR = 7.6E−05; Fig. 2C and Supplementary Table S2) and MEK–ERK signaling directly downstream of ERBB2. Moreover, it revealed a previously unknown impact of the inhibitor on the spliceosome (FDR = 7.5E−07; inset in Fig. 2C).

Resistance acquisition is accompanied by extensive reprogramming of cellular signaling

Having analyzed the impact of short-term lapatinib treatment, we next looked at signaling changes occurring upon acquisition of resistance. In line with what has been reported before (5), resistant BT-474 cells are insensitive to lapatinib treatment (EC_{50} of 4.4 μmol/L for the resistant cells and 56 nmol/L for the parental cells; Supplementary Fig. S3A), responsive to AXL inhibition (EC_{50} of 82 nmol/L for the multikinase inhibitor BMS-777607, which also targets AXL; Supplementary Fig. S3B), and have a proliferation rate comparable with the parental cells (Supplementary Fig. S3C). As AXL expression was found to be directly dependent on the selective pressure of lapatinib, the growth medium of the resistant cell line was supplemented with 1 μmol/L lapatinib throughout the study (Supplementary Fig. S3D).

Global proteome and phosphoproteome analysis of resistant versus parental cells showed that 767 out of 6,318 proteins (247 up and 521 down; Supplementary Fig. S3E) and 2,247 out of 6421 phosphorylation sites (1,111 up and 1,136 down; Fig. 3A) changed significantly. The latter corresponds to over one third of all covered sites, which is surprisingly large in comparison with the moderate changes elicited by short-term

Published OnlineFirst February 16, 2017; DOI: 10.1158/0008-5472.CAN-16-2976

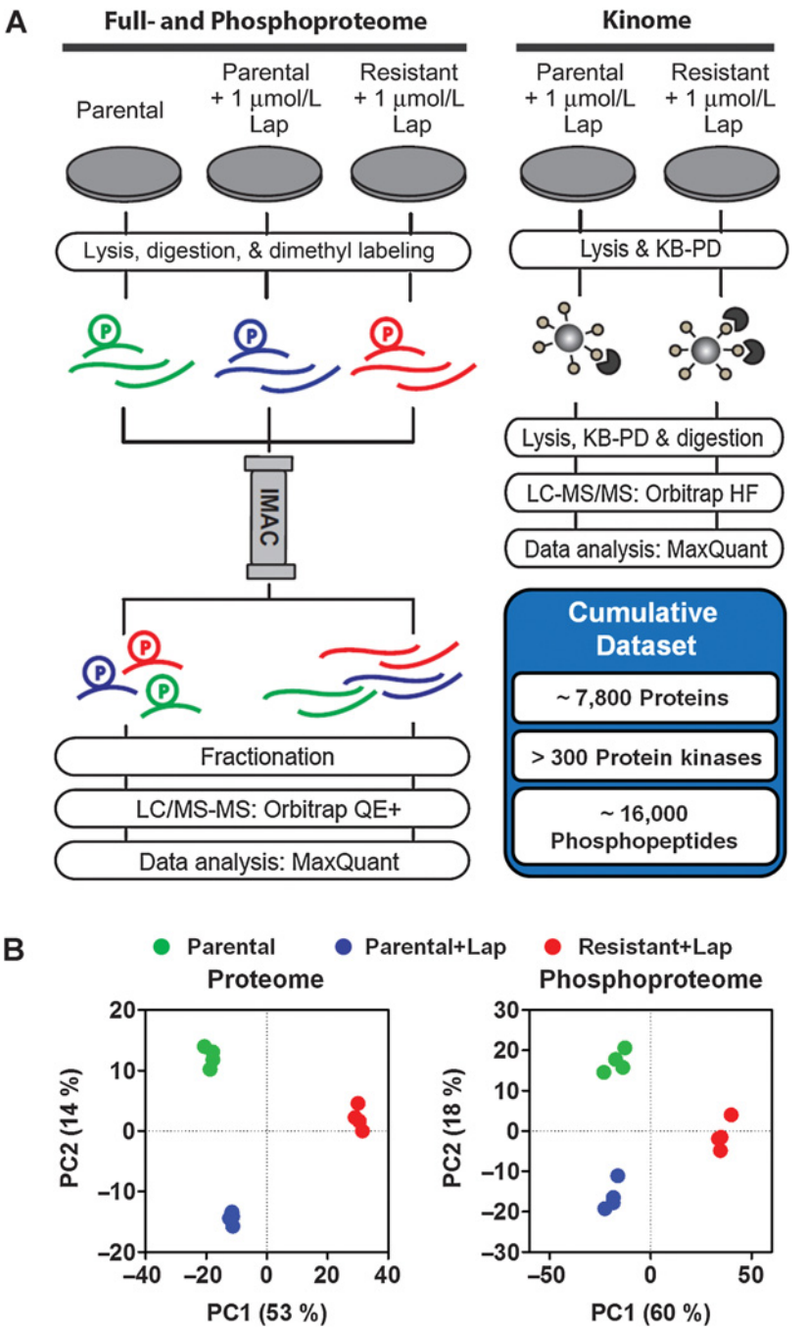

Figure 1.

Multiproteomic characterization of lapatinib treatment in parental BT-474 cells (parental) and their resistant counterpart BT-474-J4 (resistant). **A,** For the mass spectrometry–based (phospho)proteomic workflow used in this study, digested peptides from three different experimental conditions were dimethyl-labeled, combined, and enriched for phosphopeptides using Fe-IMAC chromatography. To increase proteome and phosphoproteome coverage, the column flow through was separated using hydrophilic strong anion exchange chromatography and the phosphopeptide-containing eluate was fractionated using high-pH reversed-phase microcolumns. The whole procedure was repeated in four independent biological replicates. To increase kinome coverage, kinobead pull downs were conducted in three replicates. The inset on the bottom right corner depicts the cumulative identifications of our combined dataset. **B,** PCA analysis of the three dimethyl-encoded experimental states, which were conducted in four biological replicates, shows that samples cluster tightly according to biology.

treatment with lapatinib (5% of all sites; Fig. 2A). To study signaling recovery in resistance, we divided the 332 sites that were initially inhibited by lapatinib in the parental cells into the categories "remain responsive" (182 sites), "medium recovery" (99 sites), and "strong recovery" (51 sites) according to statistical criteria and the magnitude of the $\log_2$ FC between lapatinib-treated parental and resistant cells (Supplementary Materials and Methods). Figure 3B shows protein activity indicating sites assigned to those categories. Whereas the activity of the kinases ERBB2 or MAPK1 and the transcription factors FOXO3 and BAD remained strongly inhibited, the activity of the kinases RAF1, MAPK3, GSK3A, and the transcription factor JUN recovered in lapatinib-resistant compared with sensitive cells. Globally, two-dimensional annotation enrichment (FDR < 0.01; ref. 30) confirmed the re-activation of the PIK3/AKT/MTOR signaling axis (e.g., kinases AKT, RPS6KB1, and RPS6KA1 based on combined kinase substrates and ERBB and MTOR signaling based on differential KEGG terms; Supplementary Fig. S3F; Supplementary Table S2).

As kinases are frequently involved in the resistant phenotype and contain a high proportion of pharmacologically actionable targets, kinome perturbations were of special interest.

Published OnlineFirst February 16, 2017; DOI: 10.1158/0008-5472.CAN-16-2976

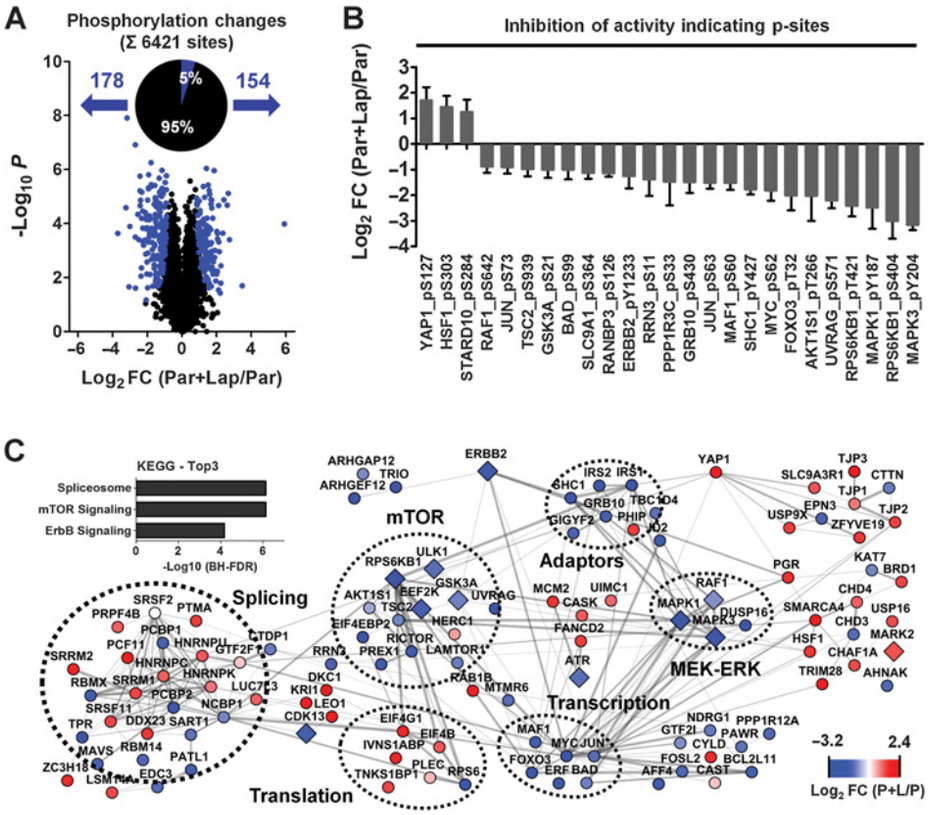

Figure 2.

(Phospho)proteomic analysis of lapatinib mode of action in parental cells. **A,** A volcano plot shows that 332 localized phosphorylation sites (found in a minimum of three biological replicates) change significantly (FDR < 0.01, S0 of 0.5; blue dots) upon 30-minute treatment with 1 μmol/L lapatinib. **B,** Bar plots display the average $\log_2$ FC of sites that are known to have a functional impact on protein activity. Among those are several sites expected to be responsive to lapatinib treatment (e.g., ERBB2 pY-1233 or SHC pY-427). **C,** Protein–protein interaction map of phosphoproteins whose sites are significantly changing upon short-term lapatinib treatment. The node color represents the $\log_2$ FC upon lapatinib treatment, whereas the thickness of the edge represents the STRING combined interaction score (>0.7). Kinases are indicated by diamond shaped nodes. Known and annotated associations are highlighted by dotted circles. The top three KEGG terms overrepresented among regulated phosphoproteins are shown in the inset. This confirms the known (inactivation of MAPK, MTOR signaling) and uncovers a new (spliceosome) mode of lapatinib action.

Complementing the phosphoproteomic data that suggested *de novo* activation of several kinases (e.g., CDK1 and SRC; Supplementary Fig. S3G), kinobead pull-downs in combination with kinome expression changes derived from the full proteome dataset confirmed the known overexpression of AXL and highlighted many other kinases with known or emerging roles in breast cancer biology [e.g., ERN1 (31), FGRF2 (32), ATR (33) and EEF2K (34), with a $\log_2$ FC of 3.1, 2.9, 2.0 and 1.9; Fig. 3C; Supplementary Table S5]. Notably, expression of the primary lapatinib targets EGFR and ERBB2 remained constant (Fig. 3C). This extensive kinome reprogramming highlights a pool of potentially relevant kinases in resistance, of which several are druggable targets.

Pharmacologic exploitation of reprogrammed cellular signaling

Our multilayered (phospho)proteomic dataset allowed us to paint a detailed molecular picture of lapatinib resistance. The pathway map depicted in Fig. 4A, summarizes both protein expression and protein phosphorylation changes in lapatinib-treated compared with resistant cells. Proteins highly overexpressed in resistance are highlighted and phosphorylation events were classified as remaining inhibited, moderately recovering, strongly recovering, or *de novo* phosphorylated depending on the fold change detected between lapatinib-treated and resistant cells (Supplementary Materials and Methods).

We next followed up on some selected observations to demonstrate the utility of such a resistance map. First, the model revealed a moderate recovery or a progressive lapatinib responsiveness of the MEK–ERK signaling branch, whereas the AKT–MTOR pathway fully recovered. In line with this, the resistant cells did not respond to treatment with the MEK inhibitor selumetinib but were exquisitely sensitive toward AKT inhibition using MK-2206 (sensitivity increases roughly 2-fold compared with parental cells; Supplementary Fig. S4A). Collectively, this suggests that our approach is capable of dissecting differentially recovering signaling nodes that can support the rational targeting of functionally relevant pathways. Application of this concept (initial responsiveness but recovery in resistance) to spliceosome phosphorylation prioritized a set of eight sites (out of the 100 sites significantly changing either upon short-term lapatinib treatment or in resistance; see

Published OnlineFirst February 16, 2017; DOI: 10.1158/0008-5472.CAN-16-2976

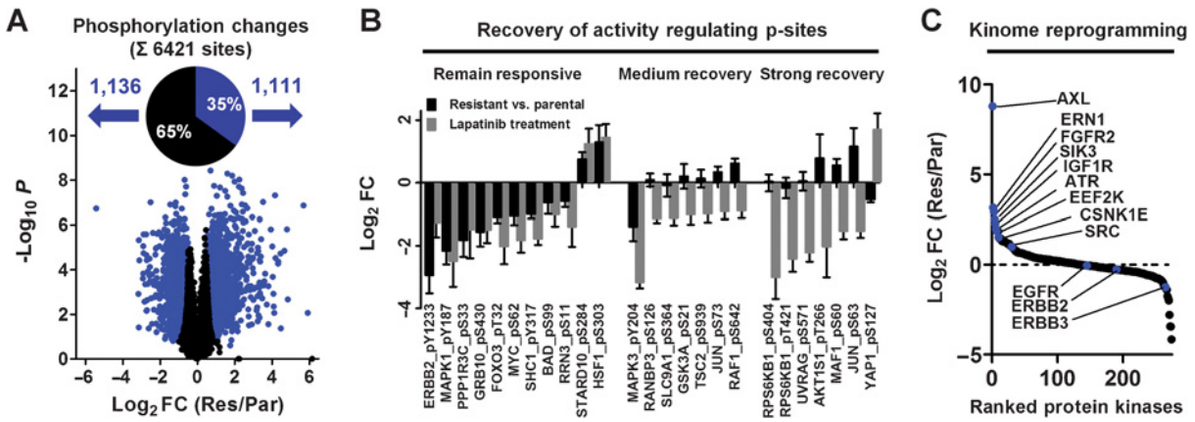

Figure 3.

Signaling reprogramming in lapatinib resistance. **A,** A volcano plot depicts significantly changing localized phosphorylation sites (found in a minimum of three biological replicates; FDR < 0.01, S0 of 0.5) in the resistant (Res) compared with the parental (Par) cell line. The magnitude of phosphoproteome alterations (35% of all sites) suggest that resistance is accompanied by a fundamental impact on tumor cell signaling. **B,** To study signaling rewiring, phosphorylation sites responsive to short-term lapatinib treatment were classified as "remain responsive" or "recovering" in resistance (depending on the magnitude of change, recovery was classified as "medium" or "strong"). The bar chart shows $\log_2$ FC of activity-associated sites from those categories in resistance and compares it with their initial $\log_2$ FC in response to short-term lapatinib treatment. **C,** Averaged quantitative kinase data from the full proteome and the affinity purification dataset were ranked according to their $\log_2$ FC between the parental (Par) and the resistant (Res) cell line.

Supplementary Table S2) on a total of six proteins that might represent a more specific means of interfering with deregulated splicing (see Table 1). Remarkably, our analysis also uncovered six cases where the expression of a specific protein isoform changed in resistance (whereas the expression of the canonical protein remained constant) and eight isoform resolving splice junction peptides with altered phosphorylation in resistance (see Table 1).

Second, we asked whether the *de novo*–activated kinases can be pharmacologically exploited. CDK1 was selected as a promising target owing to the strongest observed activation of any protein kinase present in our dataset (activity associated site pT-161 increases with a $\log_2$ FC of 2.7, Supplementary Fig. S3G). Indeed, a much higher proportion of the resistant cell population was susceptible to the CDK1 inhibitors BMS-387032 (Fig. 4C) and SCH-727965 (Supplementary Fig. S4B), which implies increased dependence on CDK1 signaling despite similar proliferation rates (Supplementary Fig. S3C).

Third and motivated by the fact that resistance against ERBB2 inhibition in breast cancer is one of the best studied model systems of resistance against targeted therapy, we asked whether common molecular drivers of resistance acquisition exist. Strikingly, our dataset contained quantitative information for virtually all of the molecules and phosphorylation events described in 20 previous studies investigating trastuzumab or lapatinib resistance in ERBB2-overexpressing breast cancer (Supplementary Fig. S4C). Whereas large-scale (phospho)proteomic measurement readily confirmed Western blot analysis–based read-outs from the same resistant cell line (e.g., *AXL* overexpression or loss of BAD pS-99 and FOXO pT-32; ref. 28) the majority of alterations found in other studies were not evident in our datasets (Supplementary Fig. S4C). However, we were able to confirm the previously described activation of *SRC* (15–17) and the overexpression of IGF1R (Supplementary Fig. S3F and S3G for SRC and Fig. 3C for IGF1R; ref. 11). Dose-dependent addition of an IGF1R inhibitor linsitinib (Supplementary Fig. S4D) or the SRC inhibitors dasatinib and saracatinib (Supplementary Fig. S4E) showed that neither of those kinases is required for proliferation in our resistance model. Owing to clear morphologic changes of the resistant cell line (Supplementary Fig. S4F) and the well-established role of the *de novo*–activated SRC in invasion (35), we additionally examined the invasive behavior in resistance and found it to be 3-fold higher compared with the parental cell line (Fig. 4D). Interestingly, the removal of lapatinib increased the invasiveness to roughly 6-fold (Supplementary Fig. S4F), which calls discontinued inhibitor exposure of patients upon the development of resistance into question. The invasive phenotype was reduced nearly back to the level of parental cells by addition of low doses of SRC inhibitors, indicating that SRC family kinases may be driving the invasiveness in resistance cells (Fig. 4D). Collectively, the obtained results suggest that resistance acquisition is molecularly very heterogeneous, that previously identified drivers of resistance can have diverse functional roles (e.g., SRC) and that activation or increased expression of proteins is not necessarily a direct indicator for functional relevance (e.g., IGF1R and proliferation).

Lapatinib resistance leads to phosphorylation-mediated changes in glycolysis

Two other described molecular mechanisms of resistance are based on glycolytic addiction caused by metabolic reprogramming (Supplementary Fig. S4C; refs. 22, 36). One of these mechanisms involves HSF1-dependent overexpression of LDHA, a metabolic protein that enhances glycolytic flux (36). Whereas LDHA was not significantly regulated in our model, we found a massive (60-fold) increase of LDAH Y-10 phosphorylation, a site that is known to cause enzymatic activation (P = 8.7E−03; Supplementary Fig. S3G; ref. 37). Also ENO1 pY-44, PKM pY-175, *PGAM1* pY-92, phosphotyrosine sites on three other important glycolytic enzymes were highly upregulated in resistance ($\log_2$ FC of 4.9, 2.8, and 3.7). In addition, several phosphoserine

Published OnlineFirst February 16, 2017; DOI: 10.1158/0008-5472.CAN-16-2976

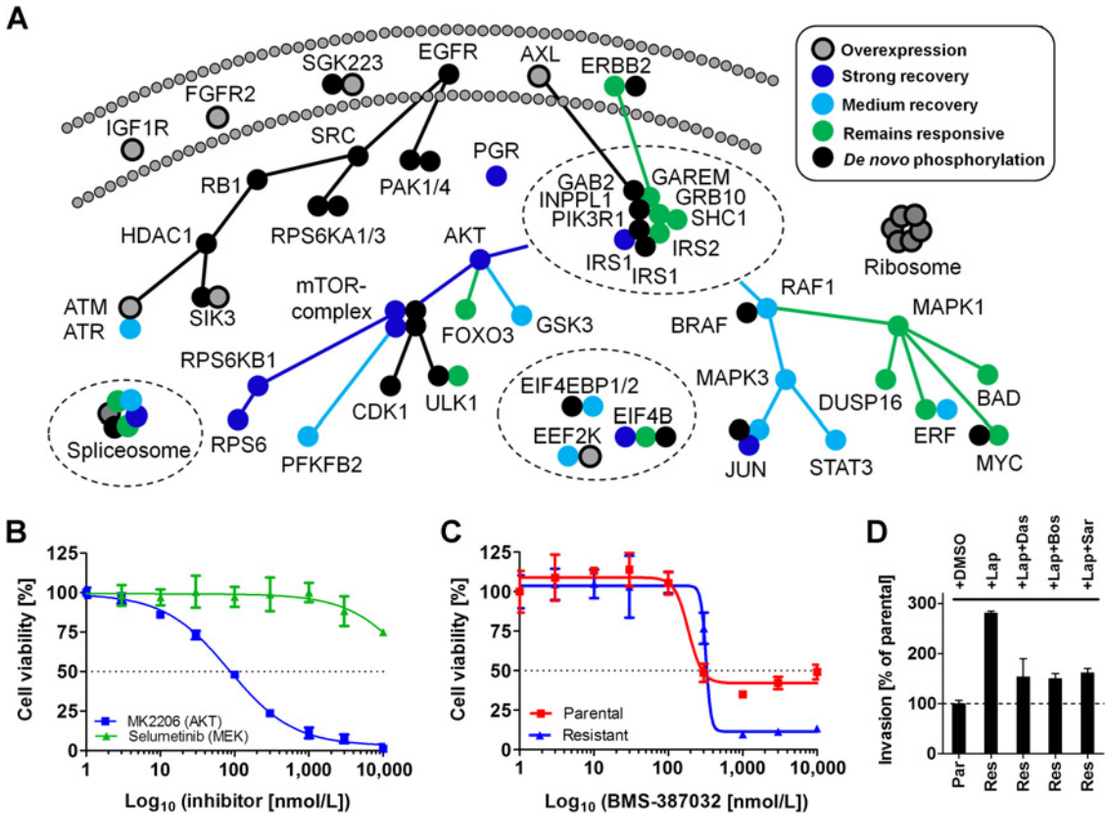

Figure 4.

Identification of pharmacologically actionable targets and phenotypes based on a breast cancer model of lapatinib resistance. **A,** A manually compiled pathway model of signaling reprogramming in resistance identifies phosphorylated nodes that remain responsive to lapatinib also in resistance (green), nodes that are reactivated and might thus reestablish proliferation (blue shades), and nodes that are *de novo*–regulated in resistance (black). Gray dots, overexpression in resistance. Different nodes/colors for the same (phospho)protein indicate that multiple such events occur simultaneously. The dotted circles highlight a strong involvement of adaptor proteins, the spliceosome, and general translational control. **B,** The extent of signaling recovery in the resistant cell line compared with the lapatinib-treated parental cell line might provide a means to prioritize pathways based on functional importance. Whereas resistant (Res) cells are not responsive to MEK inhibition, they are highly responsive to AKT inhibition. **C,** In line with strong CDK1 activation in resistance, a dose–response curve for resistant and parental cells treated with the CDK inhibitor BMS-387032 shows that a higher proportion of the resistant cell population is dependent on CDK signaling. **D,** A triplicate Matrigel invasion assay shows that resistant cells cultured in the presence of 1 μmol/L lapatinib are more invasive than their parental counterpart (cultured in 0.5% DMSO). This invasiveness can be reduced almost back to parental (Par) levels by addition of SRC inhibitors dasatinib (Das; 250 nmol/L), bosutinib (Bos; 300 nmol/L), or saracatinib (Sar; 250 nmol/L).

sites such as ALDOA pS-39, ALDOA pS-46, PFKP pS-386, and GAPDH pS-83 ($\log_2$ FC of 1.4, 1.3, 1.3, and 2.5) showed a strong gain in phosphorylation without a significant increase in protein abundance (except for ALDOA). Apart from core glycolytic enzymes, enzymes involved in glycogen catabolism were also found to be phosphorylated to a significantly higher degree in lapatinib-resistant cells compared with the parental cell line (PYGB pT-59, PGM1 pS-117, and PGM2 pS-165; $\log_2$ FC of 5.0, 2.3, and 2.1, respectively). Moreover, we observed a 1.4 $\log_2$ fold recovery of PFKFB2 pS-466 phosphorylation in resistance ($P = 5.9E{-}06$). This site was initially inhibited by lapatinib treatment and its recovery likely indicates its functional importance in resistance. Phosphorylation of pS-466 has been shown to stimulate PFKFB2 kinase activity, which catalyzes the production of fructose-2,6-bisphosphate, an allosteric activator of glycolysis (38). Finally, we observed posttranslational inactivation of PDHA1, caused by strong phosphorylation of the enzymatic activity–inhibiting sites pS-293 and pS-300 ($\log_2$ FC of 1.9 and 4.8; ref. 39). This enzyme catalyzes the conversion of pyruvate into acetyl-CoA, which is the starting point of the citric acid cycle. Taken together, these results suggested a strong, phosphorylation-mediated regulation of glucose metabolism.

To investigate whether these changes affected the levels of glycolytic metabolites, we quantitatively- and time dependently determined the levels of 86 metabolites in the resistant and parental cells 2, 8, and 24 hours after medium change (in triplicates; see Supplementary Table S6; Supplementary Fig. S5A). To summarize the obtained results and facilitate integrated analysis, we assembled the key observations from all acquired "-omics" datasets in a quantitative glycolysis map (Fig. 5A). Metabolic analysis confirmed higher intracellular levels of glucose ($\log_2$ FC of 1.9 after 8 hours) in resistant cells together with higher levels of glycolytic intermediates, which was especially apparent for glucose-6-phosphate ($\log_2$ FC of 1.6 after 8 hours), glyceraldehyde-3-phosphate ($\log_2$ FC of 1.4 after 2 hours) and phosphoenolpyruvate ($\log_2$ FC of 1.7

Published OnlineFirst February 16, 2017; DOI: 10.1158/0008-5472.CAN-16-2976

Table 1. Spliceosome phosphorylation sites recovering from lapatinib response and protein isoform–specific changes occurring in lapatinib resistance

Recovering spliceosome targets

Gene name	UniprotID	Site	Av. $\log_2$ FC (Par+Lap/Par)	Av. $\log_2$ FC (Res+Lap/Par)	Number of replicates
HNRNPU	Q00839	pS59	1.15	−0.26	4
NCBP1	Q09161	pS22	−0.98	0.08	4
PRPF4B	Q13523	pS431	1.11	−0.57	4
DDX23	Q9BUQ8	pS107	1.44	−0.17	3
SRRM2	Q9UQ35	pS1132	1.65	0.40	4
SRRM2	Q9UQ35	pS1987	1.56	0.25	4
SRRM2	Q9UQ35	pS970	1.15	−0.95	4
PCBP1	Q15365	pS264	−1.42	−0.08	4

Protein isoforms changing in resistance

Gene name	UniprotID	Protein isoform	Av. $\log_2$ FC (Res/Par)	$-\text{Log}_{10}t$ test *P*	Significant? (BH-FDR < 0.01)	Number of replicates
PDHX	O00330	Isoform 1	0.27	1.99	No	4
PDHX	O00330-2	Isoform 2	−1.02	2.78	Yes	3
HNRNPR	O43390	Isoform 1	−0.09	0.65	No	4
HNRNPR	O43390-2	Isoform 2	−0.95	4.31	Yes	4
EEF1D	P29692	Isoform 1	0.02	0.21	No	4
EEF1D	P29692-3	Isoform 3	0.95	5.76	Yes	4
DDX54	Q8TDD1-2	Isoform 2	−0.85	4.09	Yes	4
PACSIN2	Q9UNF0-2	Isoform 2	0.96	3.23	Yes	4
PPME1	Q9Y570	Isoform 1	0.25	0.50	No	4
PPME1	Q9Y570-2	Isoform 2	−1.00	5.34	Yes	4

Protein isoform–specific phosphorylation sites changing in resistance

Gene name	UniprotID	Protein isoform	Site	Av. $\log_2$ FC (Res/Par)	$-\text{Log}_{10}t$ test *P*	Number of replicates
RGS10	O43665-3	Isoform 3	pS16	−0.84	2.28	4
VAV2	P52735-3	Isoform 3	pS771	1.39	2.61	4
NDUFV3	P56181-2	Isoform 2	pS164	1.36	1.84	3
SET	Q01105-2	Isoform 2	pS15	0.78	2.44	4
PRRC2B	Q5JSZ5-5	Isoform 5	pS776	1.33	4.34	4
PRRC2B	Q5JSZ5-5	Isoform 5	pS795	1.08	3.89	4
ENAH	Q8N8S7-2	Isoform 2	pS506	2.70	3.34	4
ENAH	Q8N8S7-2	Isoform 2	pS508	2.60	2.82	4
HN1	Q9UK76-2	Isoform 2	pS88	−1.06	2.30	4
PACSIN2	Q9UNF0-2	Isoform 2	pS346	2.02	2.92	3

Abbreviations: Lap, lapatinib; Par, parental; Res, resistant.

after 8 hours; Supplementary Fig. S5A; Supplementary Table S6). Moreover, time-dependent measurement of extracellular metabolites after 8 and 24 hours revealed that the resistant cells import higher amounts of glucose, export more lactate, and massively secrete pyruvate compared with their parental counterpart (Fig. 5B; Supplementary Table S6). Collectively, the acquired intracellular and extracellular metabolomic data clearly provide compelling evidence for a higher glycolytic activity, which supports conclusions drawn from phosphorylation changes.

Finally, we investigated whether the increased glycolytic activity in resistant cells can be therapeutically exploited. Hence, we treated resistant and parental cells with the competitive hexokinase inhibitor 2-deoxy glucose. Figure 5C shows that the resistant cells were indeed more sensitive to glycolysis inhibition by 2-deoxy-glucose (2-DO-Glc), in line with our metabolomic and phosphoproteomic results. Importantly, glycolysis inhibitors such as 2-DO-Glc or the antidiabetic drug metformin, which restricts glucose availability, are actively evaluated in clinical breast cancer trials that render their application a viable therapeutic option.

Discussion

In this study, we used a multilayered proteomic approach to investigate how the small-molecule kinase inhibitor lapatinib acts on responsive, ERBB2-overexpressing breast cancer cells and compared this to the rewired signaling of lapatinib-resistant cells. This setup allowed us to functionally prioritize phosphorylation site and pathway changes in resistance in light of their initial responsiveness to lapatinib, with the rational that re-activation of initially inhibited pathways must be crucial for the resistant phenotype. Collectively, the data confirmed previous observations made using classical biochemical approaches (e.g., PIK3-AKT-MTOR recovery or AXL overexpression; ref. 5), but also provided many new additional molecular insights, of which we are only able to discuss a few.

First, splicing was shown to be heavily affected by short-term lapatinib treatment of parental cells. Splicing is already well known to be implicated in virtually all steps of tumor biology and is frequently involved in oncogenic transformation. Hence, the spliceosome is increasingly recognized as druggable tumor target (40) and specifically so in ERBB2-overexpressing breast cancer (41). Moreover, spliceostatins (or analogues thereof) are known to inhibit parental BT-474 cells with low nanomolar affinity (42). Specifically, we found three sites of the direct spliceostatin A target SF3B to be responsive to lapatinib (43). Impairment of splicing mechanisms might thus represent a previously unrecognized mechanism of lapatinib action in breast cancer. Our analysis also prioritized a set of specific, splicing-related targets based on differential expression of protein isoforms and based on initially responsive sites whose phosphorylation is restored in resistance. Interestingly, one of those proteins is the

Published OnlineFirst February 16, 2017; DOI: 10.1158/0008-5472.CAN-16-2976

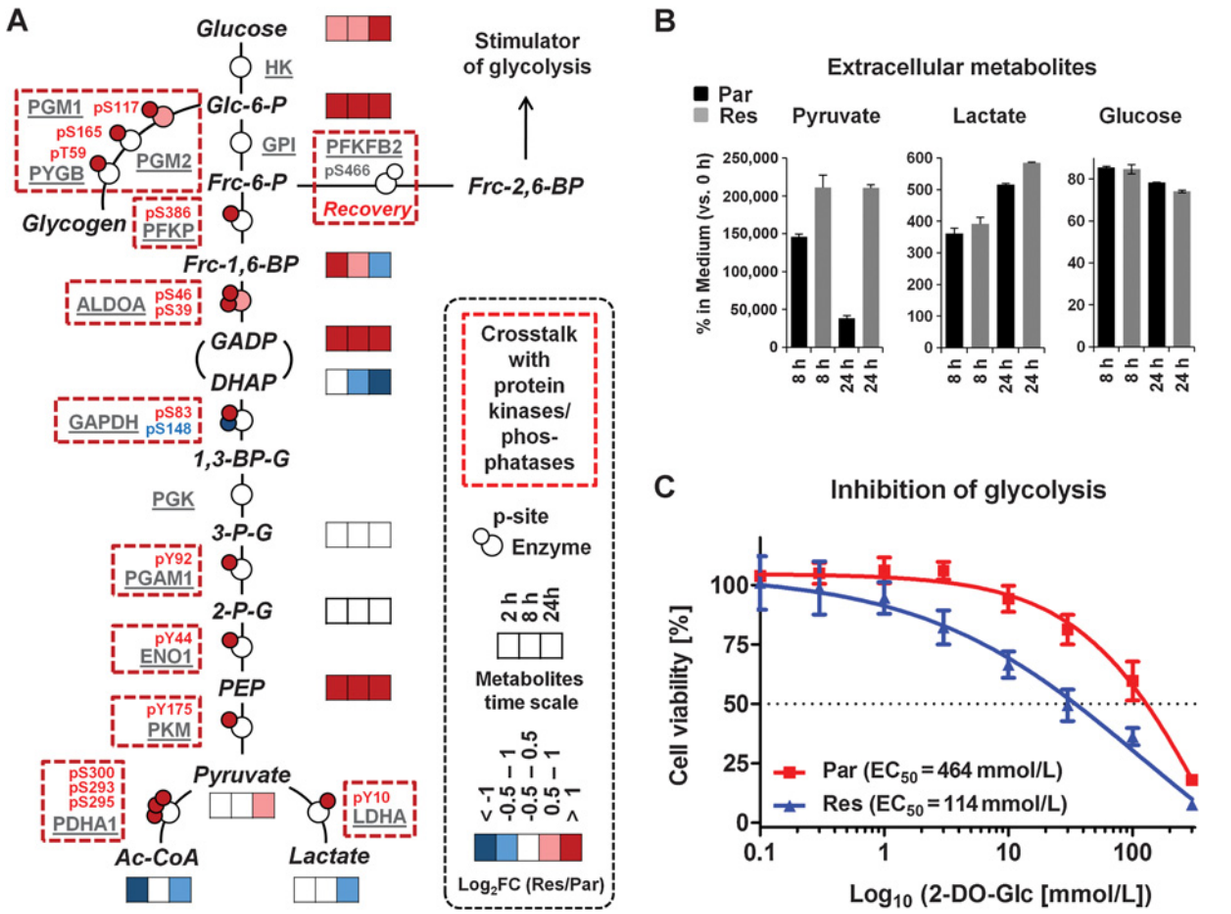

Figure 5.

Phosphorylation-mediated rewiring of glycolysis as a targetable alteration in lapatinib-resistant breast cancer cells. **A,** A metabolic pathway model summarizes expression (significant with a FDR < 0.01), phosphorylation (significant with a FDR < 0.01), and time-dependent (after 2, 8, and 24 hours) metabolite changes of resistant (Res) and parental (Par) cells. Big dots, metabolic enzymes; small dots, phosphorylation sites. The color code indicating magnitude of FC is consistent for all data types. The absence of protein expression changes suggests that glycolytic rewiring is driven by phosphorylation on a posttranslational level. Phosphorylation affects many known glycolytic enzymes that provide widespread evidence for cross-talk with oncogenic protein kinases and/or phosphatases (red boxes). **B,** Metabolite levels present in media of resistant (Res) and parental (Par) cells were determined after 8 and 24 hours. **C,** Compared with the parental cell line, the resistant cells show a decreased viability upon treatment with increasing doses of 2-deoxy-glucose (2-DO-Glc) for 96 hours.

serine/threonine-protein kinase PRP4 homolog, which has recently been implicated in ESR1 signaling and taxane response in ER^+ breast cancer (44) and has been shown to be regulated by ERBB2 in breast cancer cells (45).

Second, the data allowed us to propose a detailed model of signaling adaptor rewiring in resistance. Reestablished phosphorylation might imply a higher relevance of IRS1, GAB2, and INPPL1 for resistance acquisition as compared with several other adaptor proteins that remain dephosphorylated (e.g., SHC1 or IRS2). Whereas GAB2 pY-452 is known to confer resistance against BCR/ABL–targeted therapy, we found GAB2 pY-476 to be important in AXL-mediated resistance [the site is not responsive to short-term lapatinib treatment, highly upregulated in resistance, and known to induce interaction with PIK3R1, the regulatory subunit of PIK3 (46)]. *GAB2* is an amplifier of oncogenic signaling, serves as a signaling integrator, and also confers imatinib resistance in chronic myeloid leukemia, which might make it an ideal target for the effective treatment of a diverse set of cancers addicted to deregulated RTKs (47). The same applies to IRS1 and INPPL1, which are known to confer the mitogenic signals of several oncoproteins and have potential therapeutic value (48, 49).

Third, the integrative data analysis suggests that the cell tries to surmount initial inhibitor action by excessive re-activation of initially targeted nodes and pathways (e.g., the spliceosome; Supplementary Fig. S5B), the hormone receptor PGR or the translation-associated kinase EEF2K. Hence, our analysis also singles out phosphorylation sites that might be useful as early markers of resistance onset. The immediate upregulation of the *PGR* transcription inducing site pS-102 indicates a direct and posttranslational link between lapatinib action and PGR activation, which further emphasizes the emerging paradigm of ERBB2–PGR cross-talk (50). The fact that this activity is lost in resistance (probably at least in part due the loss of *PGR* expression itself) makes it intriguing to speculate that PGR activity needs to be

Published OnlineFirst February 16, 2017; DOI: 10.1158/0008-5472.CAN-16-2976

low to ensure proper survival of ERBB2-overexpressing breast cancer cells.

Fourth, lapatinib treatment of sensitive BT-474 cells is known to affect glycolysis (22) and our analysis unveiled that phosphorylation of S-466 on PFKFB2, a regulator indirectly affecting a rate-limiting step in glycolysis, is inhibited in response to lapatinib treatment but is recovering to initial phosphorylation levels (i.e., to the same extent as nontreated parental cells) in resistance, providing a molecular connection between lapatinib mode of action and therapeutically relevant metabolic reprogramming in resistance. This specific example shows that the analysis of the initial drug mode of action is crucial for the interpretation of phosphorylation changes in resistance, as this observation would have gone unnoticed if parental cells would be compared with resistant cells directly.

Our study demonstrates that resistance in our cell line is characterized by extensive posttranslational changes on glycolytic enzymes. Importantly, the fact that this reprogramming was not apparent from protein expression changes underscores the importance to study posttranslational events in general and phosphorylation in particular. Moreover, metabolic alterations are an established hallmark of cancer and phosphorylation is emerging as a major switch connecting oncogenic protein kinase signaling to modified metabolic activity (51). Indeed, we found many examples where phosphorylation on metabolic enzymes cooccurs with the expected shift of metabolite levels. For example, phosphorylation of PDHA1 at S-293/S-300, which is known to inhibit its enzymatic activity (39), is codetected with a decrease in intracellular Acetyl-CoA abundance and a concomitant secretion of pyruvate. The latter might additionally be promoted by a strong increase in Y-175 phosphorylation of PKM, which is responsible for pyruvate production. PKM is particularly interesting, as it is one of the rate-limiting enzymes in glycolysis and well known to be controlled by kinase signaling (52). Another example is pY-44 of ENO1, which cooccurs with strong and sustained elevation of its enzymatic product 2-phosphoglycerate. Our analysis further uncovered a massive increase in intracellular glucose-6-phosphate levels and phosphorylation of several key enzymes responsible for glycogenolysis (which ultimately results in glucose-6-phosphate production). This might be another way for the resistant cells to fuel glycolysis, which can be targeted.

Some of the detected phosphorylation sites have previously been connected to specific oncogenic kinases. As mentioned above, LDHA Y-10 is known to be phosphorylated by several tyrosine kinases [e.g., FGFR or ABL (37)]. Activated *SRC* is capable of phosphorylating ENO1 and PGAM1 and PDHA1 S-293 and S-300 are known to be phosphorylated by PDK isoenzymes (53, 39). Other sites on glycolytic enzymes (e.g., PFKP pS-386, GAPDH pS-83) are not yet associated with a specific kinase/phosphatase and provide starting points for further analysis of kinase-mediated metabolic control. Overall, the extent of glycolytic rewiring, the occurrence of various phosphoserine/-threonine as well as phosphotyrosine sites, and the diversity of functionally involved kinases suggest that posttranslational-mediated glycolytic addiction is a collective phenomenon rather than being caused by one single kinase.

Metabolic alterations are increasingly implicated in resistance against kinase inhibitors in general and lapatinib in particular (22–24). Importantly though, all previously described mechanisms are dependent on expression changes. To the best of our knowledge, this is the first study to show that such a metabolic shift involved in lapatinib resistance can occur exclusively by change of enzymatic activity, which is likely caused by posttranslational regulation. Interestingly, recent reports suggest that metabolites are themselves capable of affecting kinase pathways. For example, lactate, which is found to accumulate in our resistant cell line, has been shown to engage AXL and activate the PIK3 pathway (54). This reciprocal cross-talk might open up exciting new therapeutic opportunities and shows how important it is to understand resistance on a systems-wide level.

Furthermore, our proteomic datasets revealed that mechanisms of resistance acquisition are very heterogeneous and that previously identified resistance drivers can result in different phenotypic changes, depending on the resistant cell line used. This heterogeneity might pose a great challenge in terms of unifying treatment options. Thus, it might be a more efficient strategy to search for common alterations and molecular integrators of different, heterogeneous resistance mechanisms. As an example, several resistance mechanisms observed in ERBB2-overexpressing breast cancer, whether it is AXL, EPHA2, or MET, lead to the reactivation of PIK3, which might consequently be a more attractive node to target (5, 9, 12). Glycolysis is another example: both, our cell line and the resistant cell line from Komurov and colleagues, are sensitive to inhibition of the glycolysis rate-limiting enzyme hexokinase via 2-deoxy glucose treatment independent of the way glycolytic addiction has been acquired (22). Moreover, recent reports also establish a link between hormone receptor overexpression, altered metabolism, MTOR signaling, and lapatinib resistance (23, 24). Although all three aberrations represent individually targetable entities, they seem to depend on each other. Indeed, also in our cell line model estrogen receptor upregulation is responsible for AXL overexpression as shown by Liu and colleagues (5). This interplay between different molecular aberrations implies that there are diverse ways of targeting the resistant phenotype. Selecting the mechanism most commonly occurring might thus emerge as a key step in resistance management.

Finally, our dataset contains many additional observations (e.g., multiple deregulated intracellular/extracellular metabolites, signaling events and kinase targets). For example, we observed a massive secretion of the acidic metabolite glutamate, which is known to promote growth and invasion (55). Given the prevalence of brain metastasis in breast cancer and the observed invasive phenotype connected to lapatinib resistance, knowledge about potential metabolic mechanisms causing or amplifying invasion might ultimately result in better cure of disease. In addition, not only glycolysis is deregulated but we rather find a strong global impact of resistance acquisition on diverse metabolic pathways such as the citric acid cycle, redox signaling, amino acid metabolism, and several more (Supplementary Fig. S5A). These and other findings clearly merit closer inspection, which places this work as a rich resource for further studies.

Disclosure of Potential Conflicts of Interest

B. Kuster has ownership interest (including patents) in OmicScouts and is a consultant/advisory board member for OmicScouts. No potential conflicts of interest were disclosed by the other authors.

Authors' Contributions

Conception and design: B. Ruprecht, S. Lemeer
Development of methodology: B. Ruprecht, S. Lemeer

Published OnlineFirst February 16, 2017; DOI: 10.1158/0008-5472.CAN-16-2976

Acquisition of data (provided animals, acquired and managed patients, provided facilities, etc.): B. Ruprecht, E.A. Zaal, W. Wu, C.R. Berkers, S. Lemeer
Analysis and interpretation of data (e.g., statistical analysis, biostatistics, computational analysis): B. Ruprecht, E.A. Zaal, J. Zecha, C.R. Berkers, B. Kuster, S. Lemeer
Writing, review, and/or revision of the manuscript: B. Ruprecht, E.A. Zaal, J. Zecha, W. Wu, C.R. Berkers, B. Kuster, S. Lemeer
Administrative, technical, or material support (i.e., reporting or organizing data, constructing databases): B. Ruprecht, J. Zecha
Study supervision: B. Kuster, S. Lemeer

Acknowledgments

The authors would like to express their sincere gratitude to Andrea Hubauer for excellent technical assistance and the Department of Translational Research, GlaxoSmithKline for kindly providing the lapatinib-resistant and parental cell line. Moreover, we would like to thank Hannes Hahne and Daniel Zolg for support with data normalization and Stephanie Heinzlmeir for helpful suggestions and critical reading of the manuscript.

Grant Support

This work was in part funded by the Center for Integrated Protein Science Munich (CIPSM). S. Lemeer acknowledges support from the Netherlands Organization for Scientific Research (NWO) through a VIDI grant (project 723.013.008). C.R. Berkers acknowledges support from the Netherlands Organization for Scientific Research (NWO) through a VENI grant (project 722.013.009).

The costs of publication of this article were defrayed in part by the payment of page charges. This article must therefore be hereby marked *advertisement* in accordance with 18 U.S.C. Section 1734 solely to indicate this fact.

Received November 9, 2016; revised January 19, 2017; accepted January 24, 2017; published OnlineFirst February 16, 2017.

References

1. Slamon DJ, Clark GM, Wong SG, Levin WJ, Ullrich A, McGuire WL. Human breast cancer: correlation of relapse and survival with amplification of the HER-2/neu oncogene. Science 1987;235:177–82.
2. Fiore PD, Pierce JH, Kraus MH, Segatto O, King CR, Aaronson SA. erbB-2 is a potent oncogene when overexpressed in NIH/3T3 cells. Science 1987;237:178–82.
3. Slamon DJ, Leyland-Jones B, Shak S, Fuchs H, Paton V, Bajamonde A, et al. Use of chemotherapy plus a monoclonal antibody against HER2 for metastatic breast cancer that overexpresses HER2. N Engl J Med 2001;344:783–92.
4. Geyer CE, Forster J, Lindquist D, Chan S, Romieu CG, Pienkowski T, et al. Lapatinib plus capecitabine for HER2-positive advanced breast cancer. N Engl J Med 2006;355:2733–43.
5. Liu L, Greger J, Shi H, Liu Y, Greshock J, Annan R, et al. Novel mechanism of lapatinib resistance in HER2-positive breast tumor cells: activation of AXL. Cancer Res 2009;69:6871–8.
6. Ritter CA, Perez-Torres M, Rinehart C, Guix M, Dugger T, Engelman JA, et al. Human breast cancer cells selected for resistance to trastuzumab in vivo overexpress epidermal growth factor receptor and ErbB ligands and remain dependent on the ErbB receptor network. Clin Cancer Res 2007;13:4909–19.
7. Garrett JT, Olivares MG, Rinehart C, Granja-Ingram ND, Sánchez V, Chakrabarty A, et al. Transcriptional and posttranslational up-regulation of HER3 (ErbB3) compensates for inhibition of the HER2 tyrosine kinase. Proc Natl Acad Sci 2011;108:5021–6.
8. Canfield K, Li J, Wilkins OM, Morrison MM, Ung M, Wells W, et al. Receptor tyrosine kinase ERBB4 mediates acquired resistance to ERBB2 inhibitors in breast cancer cells. Cell Cycle 2015;14:648–55.
9. Zhuang G, Brantley-Sieders DM, Vaught D, Yu J, Xie L, Wells S, et al. Elevation of receptor tyrosine kinase EphA2 mediates resistance to trastuzumab therapy. Cancer Res 2010;70:299–308.
10. Nahta R, Yuan LXH, Zhang B, Kobayashi R, Esteva FJ. Insulin-like growth factor-I receptor/human epidermal growth factor receptor 2 heterodimerization contributes to trastuzumab resistance of breast cancer cells. Cancer Res 2005;65:11118–28.
11. Lu Y, Zi X, Zhao Y, Mascarenhas D, Pollak M. Insulin-like growth factor-I receptor signaling and resistance to trastuzumab (Herceptin). J Natl Cancer Inst 2001;93:1852–7.
12. Shattuck DL, Miller JK, Carraway KL, Sweeney C. Met receptor contributes to trastuzumab resistance of Her2-overexpressing breast cancer cells. Cancer Res 2008;68:1471–7.
13. Wang Q, Quan H, Zhao J, Xie C, Wang L, Lou L. RON confers lapatinib resistance in HER2-positive breast cancer cells. Cancer Lett 2013;340:43–50.
14. Moody SE, Schinzel AC, Singh S, Izzo F, Strickland MR, Luo L, et al. PRKACA mediates resistance to HER2-targeted therapy in breast cancer cells and restores anti-apoptotic signaling. Oncogene 2015;34:2061–71.
15. De Luca A, D'Alessio A, Gallo M, Maiello MR, Bode AM, Normanno N. Src and CXCR4 are involved in the invasiveness of breast cancer cells with acquired resistance to lapatinib. Cell Cycle 2013;13:148–56.
16. Rexer BN, Ham A-JL, Rinehart C, Hill S, Granja-Ingram Nde M, González-Angulo AM, et al. Phosphoproteomic mass spectrometry profiling links Src family kinases to escape from HER2 tyrosine kinase inhibition. Oncogene 2011;30:4163–74.
17. Zhang S, Huang W-C, Li P, Guo H, Poh S-B, Brady SW, et al. Combating trastuzumab resistance by targeting SRC, a common node downstream of multiple resistance pathways. Nat Med 2011;17:461–9.
18. Campbell IG, Russell SE, Choong DYH, Montgomery KG, Ciavarella ML, Hooi CSF, et al. Mutation of the PIK3CA gene in ovarian and breast cancer. Cancer Res 2004;64:7678–81.
19. Nahta R, Takahashi T, Ueno NT, Hung M-C, Esteva FJ. P27kip1 down-regulation is associated with trastuzumab resistance in breast cancer cells. Cancer Res 2004;64:3981–6.
20. Xia W, Bacus S, Hegde P, Husain I, Strum J, Liu L, et al. A model of acquired autoresistance to a potent ErbB2 tyrosine kinase inhibitor and a therapeutic strategy to prevent its onset in breast cancer. Proc Natl Acad Sci 2006;103:7795–800.
21. Zhao Y, Liu H, Liu Z, Ding Y, LeDoux SP, Wilson GL, et al. Overcoming trastuzumab resistance in breast cancer by targeting dysregulated glucose metabolism. Cancer Res 2011;71:4585–97.
22. Komurov K, Tseng J-T, Muller M, Seviour EG, Moss TJ, Yang L, et al. The glucosedeprivation network counteracts lapatinibinduced toxicity in resistant ErbB2positive breast cancer cells. Mol Syst Biol 2012;8:596.
23. Deblois G, Smith HW, Tam IS, Gravel S-P, Caron M, Savage P, et al. ERRα mediates metabolic adaptations driving lapatinib resistance in breast cancer. Nat Commun 2016;7:12156.
24. Park S, Chang C-Y, Safi R, Liu X, Baldi R, Jasper JS, et al. ERRα-regulated lactate metabolism contributes to resistance to targeted therapies in breast cancer. Cell Rep 2016;15:323–35.
25. Boersema PJ, Raijmakers R, Lemeer S, Mohammed S, Heck AJR. Multiplex peptide stable isotope dimethyl labeling for quantitative proteomics. Nat Protoc 2009;4:484–94.
26. Ruprecht B, Koch H, Medard G, Mundt M, Kuster B, Lemeer S. Comprehensive and reproducible phosphopeptide enrichment using iron immobilized metal ion affinity chromatography (Fe-IMAC) columns. Mol Cell Proteomics 2015;14:205–15.
27. Médard G, Pachl F, Ruprecht B, Klaeger S, Heinzlmeir S, Helm D, et al. Optimized chemical proteomics assay for kinase inhibitor profiling. J Proteome Res 2015;14:1574–86.
28. Ruprecht B, Zecha J, Heinzlmeir S, Médard G, Lemeer S, Kuster B. Evaluation of kinase activity profiling using chemical proteomics. ACS Chem Biol 2015;10:2743–52.
29. Cox J, Mann M. MaxQuant enables high peptide identification rates, individualized p.p.b.-range mass accuracies and proteome-wide protein quantification. Nat Biotechnol 2008;26:1367–72.

30. Tyanova S, Temu T, Sinitcyn P, Carlson A, Hein MY, Geiger T, et al. The Perseus computational platform for comprehensive analysis of (prote) omics data. Nat Methods 2016;13:731–40.
31. Rajapaksa G, Nikolos F, Bado I, Clarke R, Gustafsson J-Å, Thomas C. ERβ decreases breast cancer cell survival by regulating the IRE1/XBP-1 pathway. Oncogene 2015;34:4130–41.
32. Wei W, Liu W, Serra S, Asa SL, Ezzat S. The breast cancer susceptibility FGFR2 provides an alternate mode of HER2 activation. Oncogene. 2015 Feb 2. [Epub ahead of print].
33. Abdel-Fatah TMA, Middleton FK, Arora A, Agarwal D, Chen T, Moseley PM, et al. Untangling the ATR-CHEK1 network for prognostication, prediction and therapeutic target validation in breast cancer. Mol Oncol 2015;9:569–85.
34. Yao Z, Li J, Liu Z, Zheng L, Fan N, Zhang Y, et al. Integrative bioinformatics and proteomics-based discovery of an eEF2K inhibitor (cefatrizine) with ER stress modulation in breast cancer cells. Mol Biosyst 2016;12:729–36.
35. Guarino M. Src signaling in cancer invasion. J Cell Physiol 2010;223: 14–26.
36. Zhao YH, Zhou M, Liu H, Ding Y, Khong HT, Yu D, et al. Upregulation of lactate dehydrogenase A by ErbB2 through heat shock factor 1 promotes breast cancer cell glycolysis and growth. Oncogene 2009;28:3689–701.
37. Fan J, Hitosugi T, Chung T-W, Xie J, Ge Q, Gu T-L, et al. Tyrosine phosphorylation of lactate dehydrogenase A is important for NADH/ NAD(+) redox homeostasis in cancer cells. Mol Cell Biol 2011;31: 4938–50.
38. Marsin AS, Bertrand L, Rider MH, Deprez J, Beauloye C, Vincent MF, et al. Phosphorylation and activation of heart PFK-2 by AMPK has a role in the stimulation of glycolysis during ischaemia. Curr Biol CB 2000; 10:1247–55.
39. Korotchkina LG, Patel MS. Probing the mechanism of inactivation of human pyruvate dehydrogenase by phosphorylation of three sites. J Biol Chem 2001;276:5731–8.
40. van Alphen RJ, Wiemer EA, Burger H, Eskens FA. The spliceosome as target for anticancer treatment. Br J Cancer 2008;100:228–32.
41. Menon R, Omenn GS. Proteomic characterization of novel alternative splice variant proteins in human epidermal growth factor receptor 2/neu-induced breast cancers. Cancer Res 2010;70:3440–9.
42. Eustáquio AS, Janso JE, Ratnayake AS, O'Donnell CJ, Koehn FE. Spliceostatin hemiketal biosynthesis in Burkholderia spp. is catalyzed by an iron/α-ketoglutarate–dependent dioxygenase. Proc Natl Acad Sci U S A 2014; 111:E3376–85.
43. Kaida D, Motoyoshi H, Tashiro E, Nojima T, Hagiwara M, Ishigami K, et al. Spliceostatin A targets SF3b and inhibits both splicing and nuclear retention of pre-mRNA. Nat Chem Biol 2007;3:576–83.
44. Lahsaee S, Corkery DP, Anthes LE, Holly A, Dellaire G. Estrogen receptor alpha (ESR1)-signaling regulates the expression of the taxane-response biomarker PRP4K. Exp Cell Res 2016;340:125–31.
45. Corkery DP, Le Page C, Meunier L, Provencher D, Mes-Masson A-M, Dellaire G. PRP4K is a HER2-regulated modifier of taxane sensitivity. Cell Cycle 2015;14:1059–69.
46. Crouin C, Arnaud M, Gesbert F, Camonis J, Bertoglio J. A yeast two-hybrid study of human p97/Gab2 interactions with its SH2 domain-containing binding partners. FEBS Lett 2001;495:148–53.
47. Wöhrle FU, Halbach S, Aumann K, Schwemmers S, Braun S, Auberger P, et al. Gab2 signaling in chronic myeloid leukemia cells confers resistance to multiple Bcr-Abl inhibitors. Leukemia 2013;27:118–29.
48. Reuveni H, Flashner-Abramson E, Steiner L, Makedonski K, Song R, Shir A, et al. Therapeutic destruction of insulin receptor substrates for cancer treatment. Cancer Res 2013;73:4383–94.
49. Suwa A, Kurama T, Shimokawa T. SHIP2 and its involvement in various diseases. Expert Opin Ther Targets 2010;14:727–37.
50. Daniel AR, Hagan CR, Lange CA. Progesterone receptor action: defining a role in breast cancer. Expert Rev Endocrinol Metab 2011;6:359–69.
51. Humphrey SJ, James DE, Mann M. Protein phosphorylation: a major switch mechanism for metabolic regulation. Trends Endocrinol Metab 2015;26:676–87.
52. Lim S-O, Li C-W, Xia W, Lee H-H, Chang S-S, Shen J, et al. EGFR signaling enhances aerobic glycolysis in triple-negative breast cancer cells to promote tumor growth and immune escape. Cancer Res 2016;76:1284–96.
53. Cooper JA, Reiss NA, Schwartz RJ, Hunter T. Three glycolytic enzymes are phosphorylated at tyrosine in cells transformed by Rous sarcoma virus. Nature 1983;302:218–23.
54. Ruan G-X, Kazlauskas A. Lactate engages receptor tyrosine kinases Axl, Tie2, and vascular endothelial growth factor receptor 2 to activate phosphoinositide 3-kinase/Akt and promote angiogenesis. J Biol Chem 2013;288: 21161–72.
55. Li L, Hanahan D. Hijacking the neuronal NMDAR signaling circuit to promote tumor growth and invasion. Cell 2013;153:86–100.

Published OnlineFirst February 16, 2017; DOI: 10.1158/0008-5472.CAN-16-2976

Cancer Research
The Journal of Cancer Research (1916–1930) | The American Journal of Cancer (1931–1940)

AACR American Association for Cancer Research

Lapatinib Resistance in Breast Cancer Cells Is Accompanied by Phosphorylation-Mediated Reprogramming of Glycolysis

Benjamin Ruprecht, Esther A. Zaal, Jana Zecha, et al.

Cancer Res 2017;77:1842-1853. Published OnlineFirst February 16, 2017.